GPS Solutions (2023) 27:30
https://doi.org/10.1007/s10291-022-01374-5

RESEARCH

Spatial interpolation of surface point velocity using an adaptive neuro-fuzzy inference system model: a comparative study

Seyyed Reza Ghaffari-Razin[1] · Asghar Rastbood[2] · Navid Hooshangi[1]

Received: 11 October 2022 / Accepted: 25 November 2022 / Published online: 2 December 2022

Abstract

Surface displacement measurements of the earth's crust using GNSS observations are a discrete form and occur at the location of stations. Therefore, it is not possible to study crustal deformation as a continuous field. To overcome this problem, we propose the idea of using an adaptive neuro-fuzzy inference system (ANFIS) model. In the new method, the geodetic coordinates of GPS stations are input vectors, and the components of the displacement field in two-dimensions (V_e, V_n) are used as an output. The new method is analyzed using the observations of 25 GPS stations located in the northwest of Iran. Due to ample GPS stations and a tectonically active area, this region has been selected for study. The results of the new model are compared with the GPS-observed results, and with results produced by three alternative interpolation processes, namely artificial neural network (ANN), Ordinary Kriging (OK) and polynomial velocity field. The root-mean-square error (RMSE), correlation coefficient and relative error are calculated for all four interpolation processes. In the testing step, the averaged RMSE of the ANN, ANFIS, OK, and polynomial models is 2.0, 1.6, 2.7 and 3.2 mm year. The estimated velocity field by the ANFIS has been converted to a strain field and compared to the strain obtained from GPS measurements. Comparing the modeled strains with the ANFIS and GPS output for two control stations shows a correlation coefficient of 0.94 between the new model and GPS. The results reveal the capability and efficiency of ANFIS in comparison with ANN, OK and polynomial models.

Keywords Velocity field · GPS · ANFIS · Kriging

Introduction

Currently, with the development of local and regional global navigation satellite system (GNSS) networks with proper distribution of stations, the study of tectonic movements and displacement of faults has become one of the important goals of geodesy. Analyzing and evaluating the velocity of geodetic points in a specific time and framework provides very valuable information about the tectonic movements of the earth's crust and faults. In active tectonic zones, evaluating surface displacements of the earth's crust and studying geophysical properties can reveal valuable information about geological structures. With GPS, the creation of reference points in geodetic networks has gained high speed. The important key in creating reference points is to estimate and obtain the velocity field and the displacement of these points within a reference framework (Djamour et al. 2011; Malekshahian and Raoofian-Naeeni 2018). Much research has been carried out to study the surface velocity field and geodynamic mechanisms of the crust in Iran and the world. With information about the velocity field of GPS stations in geodetic networks, the kinematics and dynamics of the earth's crust in that area can be modeled (Grafarend and Voosoghi 2003; Yilmaz 2013).

Segal and Matthews (1988) used a polynomial approximation to model the displacement field. They introduced a model coordinate solution that fixes the indeterminate components of the displacement field by minimizing the difference between the computed displacements and those predicted by a geophysical model. Chen (1991) modeled the 3-d displacement field using geodynamic data as well as the finite element method. He found that the strain pattern obtained agrees with geological structures and a completely

✉ Seyyed Reza Ghaffari-Razin
mr.ghafari@arakut.ac.ir; mirreza_ghaffari@yahoo.com

[1] Department of Geoscience Engineering, Arak University of Technology, Arāk, Iran

[2] Faculty of Civil Engineering, University of Tabriz, Tabriz, Iran

independently determined crustal uplift pattern. Voosoghi (2000) used tensor calculations to obtain a 3-d curvature tensor and a displacement field of the earth's crust. He showed surface deformation tensors and their associated invariants are being critical for a meaningful study of deformations and kinematics of the earth. Moghtased-Azar and Zaletnyik (2009) examined the capability of artificial neural networks (ANNs) in estimating the velocity field of GPS stations. They compared and evaluated the results of the ANN model with the polynomial model. Gullu et al. (2011) evaluated an interpolation method based on ANNs to estimate the velocity field. Their results showed that back-propagation ANN can be a valuable tool for estimating point velocity in the densification networks as a real alternative to the interpolation methods. Hu et al. (2012) used a variance component estimation approach to weigh the interferometric synthetic aperture radar (InSAR) and GPS measurements in deriving 3-d surface displacements. Bogusz et al. (2013) used generalized Kriging interpolation to estimate the crustal velocity field in the European region. They showed that creating a continuous velocity field in Europe will lead to obtaining the continuous strain field in future research. Yilmaz and Gullu (2014) applied two different types of ANN models for geodetic point velocity estimation. They constructed ANN models using the multilayer perceptron neural network (MLP-NN) and the radial basis function neural network (RBF-NN). Fernandez et al. (2018) reported, for the first time, the 2-d and 3-d displacement field over the study area using SAR data from Sentinel-1A images and GNSS observations. By modeling this displacement, they provided new insights on the spatial and temporal evolution of the subsidence processes and on the main governing mechanisms. Liang et al. (2021) proposed a model of annual vertical surface displacements of mainland China based on the direct observation of deformation by 234 continuous GPS stations and unified data processing using the multi-surface function method. Konakoglu (2021) investigated the predictive capacity of three MLP-NN, generalized regression neural network (GRNN) and RBF-NN models in predicting geodetic point velocities. He showed that all ANN models were able to predict the geodetic point velocity with satisfactory accuracy; however, the GRNN model provided better accuracy than the MLP-NN and RBF-NN models.

Some disadvantages can be considered for previous research in modeling and predicting the crustal deformation and surface displacement fields using GPS observations. In most studies, the estimated displacement field is point-to-point and is for the location of GPS stations. In other words, in places where there is no GPS station, the displacement field cannot be accurately checked. The previously presented models are based on analytical functions and are mostly local, i.e., accurate determination of the coefficients of these models will depend strongly on the number of observations in the study area. In models based on analytical functions, the transformation of a continuous problem into a discrete problem leads to a system of unstable equations (Hossainali et al. 2010). In these methods, the use of regularization methods to solve the system of equations is inevitable. In models based on ANN, the choice of convergence rate to the optimal solution, the number of neurons in the hidden layer, and the selection of the appropriate cost function strongly affect the accuracy of the results.

In order to overcome the limitations in the traditional models related to the prediction of the velocity field of geodetic points with GPS observations, the use of machine learning (ML) methods has been proposed. The adaptive neuro-fuzzy inference system (ANFIS) is one of the models with very high capability and efficiency for modeling and predicting the behavior of nonlinear phenomena (Yetilmezsoy 2019). The efficiency and accuracy of this method have been evaluated in various geodetic applications (Ghaffari-Razin and Voosoghi 2020; Feizi et al. 2020). Therefore, the ANFIS model is proposed as a new model to predict the crustal velocity field. The evaluation of the ANFIS is done using the observations of 25 GPS stations in the northwest of Iran. Also, the results of the new model are compared and analyzed with the velocity field obtained from GPS, ANN, Ordinary Kriging (OK), and polynomial models. Statistical analyses are performed based on the correlation coefficient, relative error and root-mean-square error (RMSE). Strain analysis is also performed using the ANFIS and is compared with the GPS-derived strain field.

Study area and observations

In order to evaluate the ANFIS model, part of northwestern Iran has been selected, which is tectonically active, includes many active faults, and has several GPS stations in the area. The occurrence of numerous large and devastating earthquakes reflects the seismicity of this region. For this reason, the study and analysis of crustal deformation and its displacement are of special importance. Observations of 25 GPS stations from 2007 to 2010 have been prepared by the Iranian National Cartographic Center (NCC). The modeling area is between 36°–40° N and 44°–49° E. The height of these stations varies from 1280 to 1952 m above sea level. Also, a choke ring antenna with a 15° cutoff angle has been used to overcome the multipath error. Figure 1 shows the study area and the velocity fields estimated by the Bernese GNSS software. Also, this figure shows the velocity vectors on the Iranian plateau relative to the Eurasian plate with a 95% confidence ellipse.

First, raw observations of all stations are processed in the Bernese GNSS software (Dach et al. 2007), and after removing various errors, the velocity vectors are

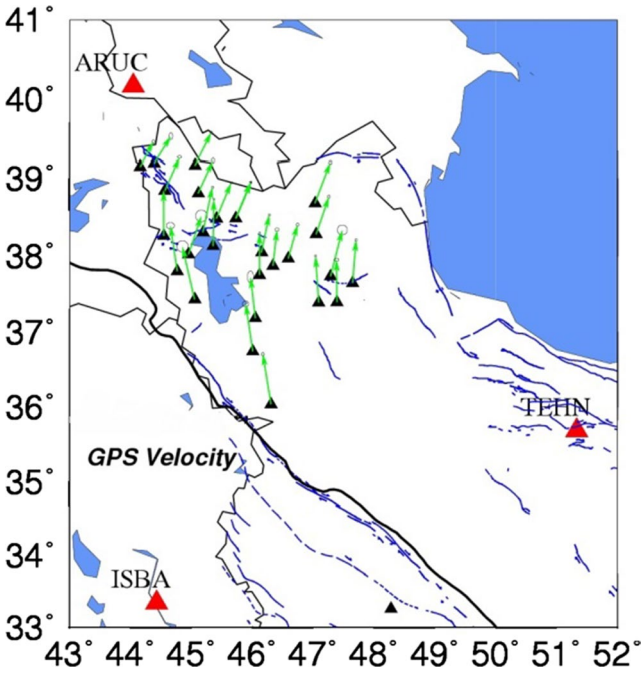

Fig. 1 Study area showing GPS velocity (green vectors), GPS situation (black triangles), IGS stations (red triangles), and major active faults in the Iranian plateau (blue lines). The velocity fields are fixed relative to the Eurasian plate. The bold black line indicates the border between the Eurasian and Arabian plates, which start in northwestern Iran and continue to the southeast

Table 1 Number of training and testing stations at three different cases for ANN and ANFIS models

	Number of training stations	Number of testing stations
Case # 1	22	3
Case # 2	18	7
Case # 3	15	10

calculated for GPS stations. Precise orbit information and earth rotation parameters have been taken from the CODE (Center for Orbit Determination in Europe). It should be noted that to define the coordinate system on the Iranian plateau and estimate the velocity vectors of GPS stations, three stations of the IGS network (ARUC, TEHN and ISBA) have been used in the processing step.

To evaluate the ANN and ANFIS models, three cases are considered for training and testing stations. These cases are performed in three modes: high, medium, and low for training stations, i.e., by reducing the number of stations used in model training, their accuracy is evaluated. Table 1 shows the number of training and testing stations in three different cases.

It should be noted that the training and testing stations were selected completely at random. The spatial distribution of training and testing stations for the three different cases is shown in Fig. 2.

The spatial distribution of the training and testing stations in the three cases is such that it can provide an accurate accuracy assessment of results obtained from the ANN and ANFIS models. The following equation shows the relationship between input and output of an ANFIS and ANN models:

$$V_{\text{ANN ANFIS}} = f(\text{Lat},\text{Lon}) \tag{1}$$

where V is the velocity field, and Lat and Lon are the latitude and longitude of GPS stations. In other words, the surface deformation analysis is based on geometrical parameters. Physical parameters are not used in deformation modeling. Figure 3 shows the diagram of the ANFIS and ANN models in the training and testing steps.

For the OK and polynomial models, the steps of the flowchart in Fig. 3 are performed, but in these two models, the least squares method is used to estimate the model coefficients. Accurate determination of the coefficients of these two models will reduce the output error and also prevent the overfitting problem.

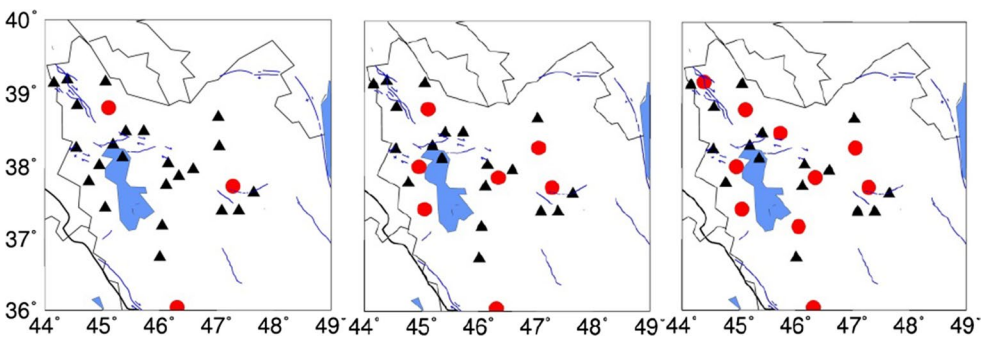

Fig. 2 Three different cases for training (black triangles) and testing stations (red circles), case # 1 (left), case # 2 (middle) and case # 3 (right) following Table 1

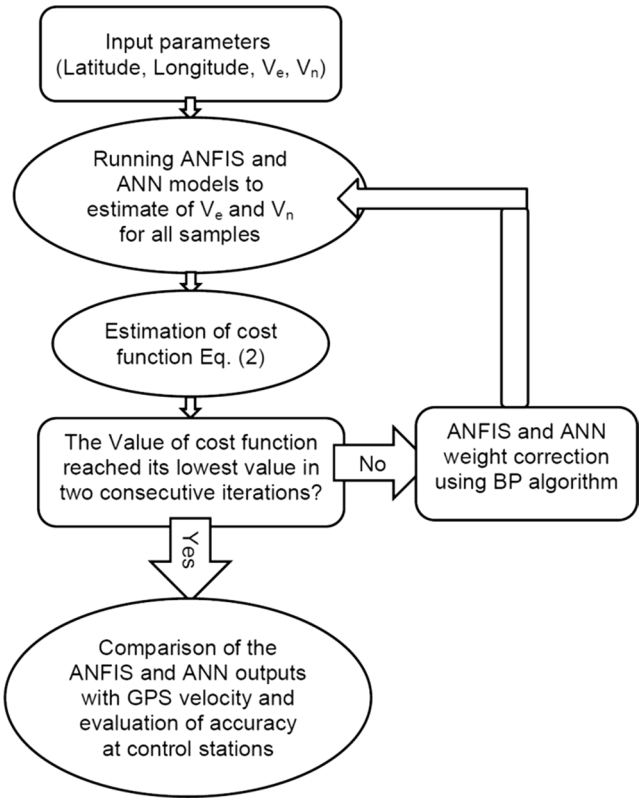

Fig. 3 Flowchart of the crustal velocity modeling and prediction using ANFIS and ANN models

Methodology

The theory of the ANFIS, Kriging, and polynomial models is presented, and their advantages and disadvantages are discussed. Also, in this section, the evaluation of the results of the models is explained. Please refer to Ghaffari Razin et al. (2015) for the ANN mathematical model.

Adaptive neuro-fuzzy inference system

An adaptive neuro-fuzzy inference system is a kind of ANN that is based on the Takagi–Sugeno fuzzy inference system. The technique was developed in the early 1990s (Jang 1993). Since it integrates both neural networks and fuzzy logic principles, it has the potential to capture the benefits of both in a single framework. Its inference system corresponds to a set of fuzzy IF–THEN rules that have the learning capability to approximate nonlinear functions. Hence, ANFIS is considered to be a universal estimator. The ANFIS architecture consists of five layers: fuzzy layer, product layer, normalized layer, defuzzy layer, and total output layer (Cakmakci et al. 2010). Figure 4 shows the mathematical relationships of the different layers of the ANFIS model.

$$\text{Layer 1} \quad Q_i^1 = \mu_{A_i}(x) = \exp\left[-\left(\frac{x-c_i}{a_i}\right)^2\right] \qquad i = 1,2$$

$$\text{Layer 2} \quad Q_i^2 = w_i = \mu_{A_i}(x) \times \mu_{B_i}(y) \qquad i = 1,2$$

$$\text{Layer 3} \quad Q_i^3 = \overline{w}_i = \frac{w_i}{w_1 + w_2} \qquad i = 1,2$$

$$\text{Layer 4} \quad Q_i^4 = \overline{w}_i f_i = \overline{w}_i (p_i x + q_i y + r_i) \qquad i = 1,2$$

$$\text{Layer 5} \quad Q_i^5 = overall \quad output = \sum_i \overline{w}_i f_i = \frac{\sum_i w_i f_i}{\sum_i w_i}$$

Fig. 4 Diagram of the mathematical relationships of the different layers of the ANFIS model

The error back-propagation (BP) algorithm is used to train the ANFIS (Rumelhart et al. 1986). This algorithm calculates the gradient of the cost function (for all the patterns) and updates the weights by moving them along the gradient-descendent direction. The cost function of the ANFIS and ANN networks is defined by

$$E = \sum_{i=1}^{N} \left(V^i_{\text{model}} - V^i_{\text{GPS}}\right)^2 \tag{2}$$

V_{model} is the modeled value of surface velocity with ANN and ANFIS, V_{GPS} is the observed value of surface velocity from GPS, and N is the number of samples.

Kriging interpolation method

The Kriging method is one of the most suitable and advanced spatial data analysis techniques. Kriging is an optimal interpolation method in which the variables are random and do not follow a specific geometric function. This method was used in the sixties by the French engineer Matheron (1971). Kriging is an unbiased estimator with the lowest estimation variance. The unbiased condition is also applied in other estimation methods, such as inverse distance and inverse distance squared, but the feature of Kriging is that it determines the unknown coefficients in such a way that the variance of the estimates is also minimal (Joseph 2006). Kriging is based on a constant mean μ for the data and random errors ε with spatial dependence as follows:

$$Z(x_0) = \mu(x_0) + \varepsilon(x_0) \tag{3}$$

where $Z(x_0)$ is the variable of interest, $\mu(x_0)$ is the deterministic trend and $\varepsilon(x_0)$ is the correlated error (Erdogan 2010). In the ordinary algorithm of Kriging, Eq. (3) can be given as follows:

$$Z(x_0) = \mu(x_0) + \sum_{i=1}^{n} \lambda_i [z(x_i) - \mu(x_0)] \tag{4}$$

where n is the number of sampled points used for the estimation, λ_i is the weight assigned to the sampled point (x_i), and $\sum_{i=1}^{n} \lambda_i = 1$ is a condition (Li and Heap 2008). Kriging is one of the most appropriate spatial interpolation methods when a spatially correlated distance or directional bias in the data is known.

Polynomial interpolation method

Using a polynomial model with multiple variables is a simple way to model the behavior of nonlinear phenomena. To estimate the velocity field at geodetic points, we used a polynomial with two spatial variables (longitude and latitude). The least squares method is also used to obtain polynomial coefficients (Ghaderpour et al. 2021). In general, a polynomial with two variables can be represented as follows (Ghaffari Razin et al. 2015):

$$V(\theta, \lambda) = \sum_{i=0}^{n} \sum_{j=0}^{n} a_{ij} \theta^i \lambda^j \tag{5}$$

V is the velocity field, θ and λ indicate the latitude and longitude of geodetic point, and a_{ij} is the unknown parameter of the polynomial. The matrix form of (5) is as follows:

$$V(\theta, \lambda) = \begin{bmatrix} 1 & \theta & \lambda & \cdots & \theta^i \lambda^j \end{bmatrix} \begin{bmatrix} a_{00} \\ a_{10} \\ \vdots \\ a_{ij} \end{bmatrix} \tag{6}$$

The necessary number of coordinates to calculate a two variables polynomial is

$$p = \frac{(r+2)(r+1)}{2} \tag{7}$$

where r is the order of the polynomial and p is the number of the necessary coordinates.

Statistical metrics

Error analysis is performed for both training and testing steps. In both steps, the RMSE, correlation coefficient (R), and relative error (RE) statistical indicators are used to evaluate the error of the models. These three indicators are defined as follows:

$$\mathrm{RMSE} = \sqrt{\frac{1}{N} \sum_{i=1}^{N} \left(V^i_{\mathrm{model}} - V^i_{\mathrm{GPS}} \right)^2} \tag{8}$$

$$R = \frac{\sum_{i=1}^{N} \left(V^i_{\mathrm{model}} - \overline{V}_i \right) \left(V^i_{\mathrm{GPS}} - \overline{V^i_{\mathrm{GPS}}} \right)}{\sqrt{\sum_{i=1}^{N} \left(V^i_{\mathrm{model}} - \overline{V}_i \right)^2} \sqrt{\sum_{i=1}^{N} \left(V^i_{\mathrm{GPS}} - \overline{V^i_{\mathrm{GPS}}} \right)}} \tag{9}$$

$$\mathrm{RE} = \left(\frac{\left(V_{\mathrm{model}} - V_{\mathrm{GPS}} \right)}{V_{\mathrm{GPS}}} \right) \times 100 \tag{10}$$

where $\overline{V}$ is the mean value of velocity field and V_{model} shows the estimated velocity field using ANN, ANFIS, OK, and polynomial models. If the value of the relative error and the RMSE are close to zero, it indicates a high accuracy of the model. The correlation coefficient indicates the degree of correlation in the output of the two models, i.e., this coefficient shows the similarity of the variations in the output of the models. The coefficient is between [0, 1], a value close to one indicates a high level of similarity between the outputs of the two models.

Results

In this section, the error analysis of the ANN, ANFIS, OK, and polynomial models is performed in the training and testing steps. In the training step, with considering the minimum RMSE, the optimal structure is selected for the ANN and ANFIS models. Also, at this step, the coefficients of the OK and polynomial models are estimated by the least squares method. After the training, the errors of the models are calculated and evaluated in the testing step.

Error analysis at the training step

Using the velocity field obtained from the training stations for three cases (Table 1), the ANN, ANFIS, OK, and polynomial models are trained. The purpose of the training step in the ANN and ANFIS is to determine the optimal structure of the networks and achieve the minimum cost function value (2). Different structures of the ANN and ANFIS are evaluated. RMSE, correlation coefficient, and convergence time to the optimal solution are calculated in these structures. Based on the minimum RMSE at the training step, the optimal structures of ANN and ANFIS models are selected. Figure 5 shows the results of this study for both the northern (V_{n}) and eastern (V_{e}) components of the velocity field for ANN and ANFIS. The number of inputs and outputs of both models is the same, so in Fig. 5, the number of hidden layer neurons

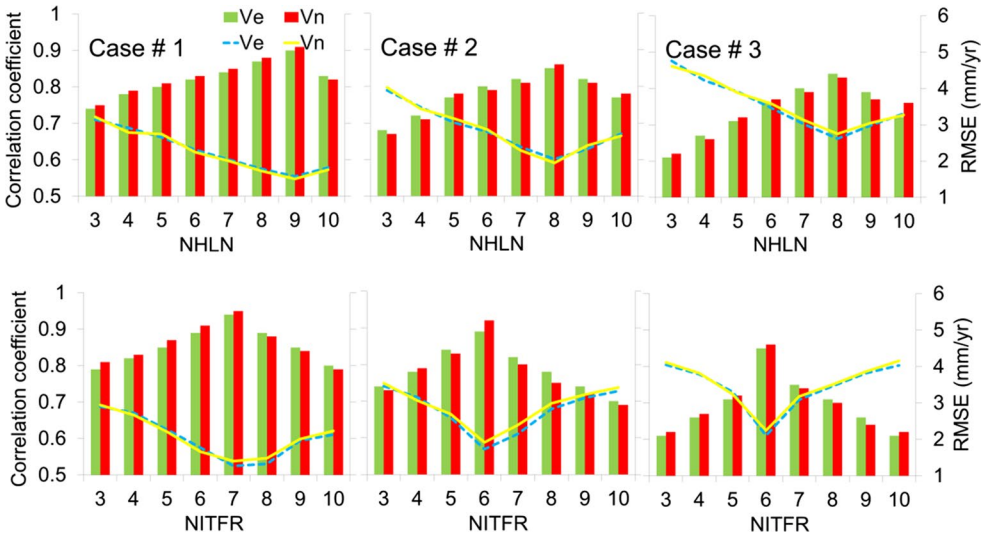

Fig. 5 Correlation coefficient (left vertical axis) and RMSE (right vertical axis) of ANN (top panel) and ANFIS (bottom panel) models in three different cases at the training step. Green and red bars show the correlation coefficient of the models; green (dashed) and yellow (continuous) curves show the RMSE (mm/year)

(NHLN) of the ANN and the number of IF–THEN fuzzy rules (NITFR) of the ANFIS model are displayed on the horizontal axis. The green and red bars show the correlation coefficient of the models, and the green (dashed) and yellow (continuous) curves show the RMSE (mm/year).

It should be noted that the modeling of the velocity field for the north and for the east directions has been done separately. This mode is also considered for the OK and polynomial models. Also, all calculations were done in a computer system with similar software and hardware. In both the ANN and ANFIS models, with the decrease in the number of training stations, the RMSE has increased. The minimum RMSE in the ANN and ANFIS in case # 1 is 1.4 and 1.2 mm, respectively. In the next two cases, the RMSE of both models in the training step is higher than that in case # 1. In both models, the optimal structure has been selected based on minimum RMSE. In the ANN and for case # 1, we select 2-9-1 as the optimal network structure. In other words, the model with nine neurons in the hidden layer has the lowest RMSE in the training step. In the ANN optimal structure of case # 1, the correlation coefficient is 0.91.

In case # 1 of the ANFIS model, the optimal value of the IF–THEN fuzzy rules is 7. In other words, the 2-7-1 is the structure with the lowest RMSE and the highest correlation coefficient in the training step. In this structure, the RMSE and correlation coefficient of the ANFIS are calculated as 1.2 mm and 0.95, respectively. Comparing the RMSE and correlation coefficient of the ANN and ANFIS models in the training step and for three cases shows that the ANFIS is more accurate than the ANN model. Even with the reduction in the number of training stations in case # 3, the ANFIS has less RMSE than the ANN model. Comparing the convergence speed of the two models in the training step shows that the ANN converges to the optimal solution faster than the ANFIS model. Both models are trained with the BP algorithm. The structure of the ANN is simpler than the ANFIS model. Therefore, the speed of calculations and convergence in this model will be faster than in the ANFIS.

The main idea of Kriging is that the closest sample points should have more weight in the prediction to improve the estimation. The weights depend on the values of the mean and the covariance function. The OK method assumes that the variance has a constant value in the entire spatial range, but its mean is unknown. The OK covariance function is valid for all spatial variations. The covariance function evaluates the quantity variations (this quantity is the surface velocity in this research) and shows that the values in two close positions have a high correlation. Choosing the variogram function is important in forecasting with the OK method. Variogram is a suitable tool for spatial data analysis. The variogram function models the spatial and temporal dependence structure of the data. The shape of the variogram function is selected using an empirical and a mathematical model based on the spatial variations in the data. The spatial variogram function ($\gamma_s(h_s)$) is obtained by calculating the variance of the variable in the neighborhood radius (h_s) of each observation point ($Z(s,t)$) from the following equations:

$$\gamma_s(h_s) = \frac{1}{2}\mathrm{Var}\left(Z(s+h_s,t) - Z(s,t)\right) \tag{11}$$

The spatial variations in the velocity field are evaluated in this research. Therefore, only the spatial variogram function is defined. Using the velocity field observations obtained from GPS in three different cases, the covariance matrix and coefficients of the OK model are estimated and then the RMSE and correlation coefficient of the training step are calculated. The results of this evaluation are shown in Table 2.

In the OK model, the RMSE in case # 1 is less than that in the other two cases. In other words, by reducing the number

Table 2 RMSE (mm/year) and correlation coefficient of OK model at three cases for northern (V_n) and eastern (V_e) components

	RMSE (mm/year)		Correlation coefficient	
	V_e	V_n	V_e	V_n
Case # 1	1.89	2.08	0.87	0.85
Case # 2	2.69	2.86	0.80	0.78
Case # 3	4.71	4.94	0.75	0.73

Table 3 RMSE (mm/year) and correlation coefficient of the quadratic polynomial model at three cases for northern (V_n) and eastern (V_e) components

	RMSE (mm/year)		correlation coefficient	
	V_e	V_n	V_e	V_n
Case # 1	2.93	3.11	0.84	0.80
Case # 2	2.56	2.89	0.85	0.81
Case # 3	2.14	2.24	0.86	0.83

of training stations in the OK model, the RMSE increases. The important point in Table 2 is that with the reduction in the number of training stations in case # 3, the RMSE of the OK model has greatly increased. This shows that the OK model RMSE depends on the number and distribution of training stations.

For the polynomial model, a model with different degrees is evaluated in three cases. The degree of the polynomial that has the lowest RMSE and the highest correlation coefficient is chosen as the optimal model. By evaluating polynomials of different degrees, we find that the polynomial of the second degree has the minimum RMSE and the highest correlation coefficient in the training step. As a result, in all three cases, a quadratic polynomial is used to estimate the components of the velocity field. Table 3 shows the RMSE and the correlation coefficient of the optimal quadratic polynomials for three cases. It should be noted that with the increase in polynomial degree, the error value of the model decreases and the correlation coefficient increases. But, as the polynomial degree increases, an overfitting problem occurs. The overfitting problem causes the modeling to deviate from its physical reality. In order to avoid overfitting problem, the polynomial model is evaluated in test stations.

The results of Table 3 show that with the decrease in the number of training stations, the RMSE of the optimal quadratic polynomial model has decreased and the correlation coefficient has increased. This shows that in the polynomial model, a large number of training stations cannot increase the accuracy of the model. In other words, in this model, the distribution of training stations is very important. For example, in case # 1, by removing one of the training stations, which has a greater distance from other training stations, the amount of RMSE in both northern and eastern components has decreased significantly. Therefore, evaluating the polynomial model at many test points can be the best solution to choose its optimal degree. The optimal quadratic polynomial coefficients for the eastern and northern components of the velocity field in all three cases are as follows:

$$V_e(\phi,\lambda) = -2708 + 34.91\phi + 84.55\lambda - 0.05\phi^2 - 0.58\phi\lambda - 0.66\lambda^2$$
$$V_n(\phi,\lambda) = 3996 - 62.55\phi - 119.4\lambda - 0.21\phi^2 + 1.65\phi\lambda + 0.60\lambda^2 \quad (12)$$

$$V_e(\phi,\lambda) = -2238 + 5.88\phi + 88.04\lambda + 0.31\phi^2 - 0.56\phi\lambda - 0.71\lambda^2$$
$$V_n(\phi,\lambda) = 3156 - 32.89\phi - 107.5\lambda - 0.52\phi^2 + 1.54\phi\lambda + 0.52\lambda^2 \quad (13)$$

$$V_e(\phi,\lambda) = -1542 - 10.38\phi + 71.38\lambda + 0.46\phi^2 - 0.46\phi\lambda - 0.57\lambda^2$$
$$V_n(\phi,\lambda) = 1839 - 8.37\phi - 70.55\lambda - 0.69\phi^2 + 1.28\phi\lambda + 0.23\lambda^2 \quad (14)$$

In these equations, ϕ and λ indicate the latitude and longitude of the GPS stations.

Error analysis at the testing step

After training the ANN, ANFIS, OK, and quadratic polynomial models in three different cases and evaluating the error of the training step, it is possible to estimate and evaluate the velocity field in the test stations (red circles in Fig. 2) with the trained models. For comparison and evaluation, the velocity field obtained from GPS is considered the reference. Figure 6 shows the relative error (%) and RMSE (mm/year) of the models in different cases. The blue and red bars show the relative error of the models, and the black (continuous) and green (dashed) curves show the RMSE.

Figure 6 shows that all four models in case # 1, which has more training stations, have less error in the testing step. In cases # 2 and 3, the error of all four models has increased. This shows that the error in the testing step increases by reducing the number of training stations. Comparing the error of four models shows the higher accuracy of the ANFIS compared to other models. The maximum and minimum relative error of the ANFIS is 6 and 10%, respectively. For the quadratic polynomial model, maximum and minimum relative errors have been calculated 14 and 24%, respectively. In the testing step and all three cases, the RMSE of the ANFIS model in both northern and eastern components is less than 2.4 mm/year. The RMSE of the ANFIS in case # 3 is lower than the RMSE of the OK and quadratic polynomial models in all three cases. In other words, the ANFIS model, with fewer training stations, has higher accuracy than the OK and quadratic polynomial models. The evaluation of the OK and quadratic polynomial models in some test stations shows that

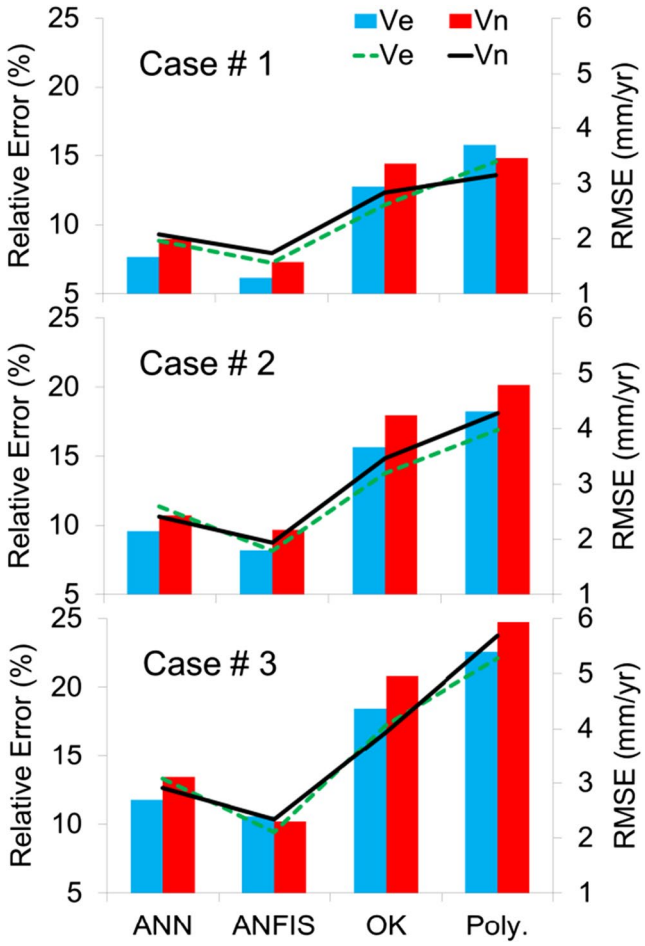

Fig. 6 Relative error (%) and RMSE (mm/year) of ANN, ANFIS, OK, and quadratic polynomial models in three different cases at the testing step. The blue and red bars are the relative error; black (continuous) and green (dashed) curves are the RMSE

as the test station moves away from the training stations, the RMSE increases greatly. In other words, in these two models, the distribution of training stations should be uniform and homogeneous so that high accuracy can be expected from the models.

Spatial interpolation of surface velocity

After evaluating the accuracy of the ANFIS, ANN, OK, and polynomial models in the training and testing steps, the velocity field can be estimated at different geodetic points and compared with the velocity field obtained from GPS. Based on the results of the testing step, the ANFIS model is more accurate compared to other models. Therefore, this section compares the results for the velocity field obtained from this model. Figure 7 shows the velocity field estimated by the ANFIS model in the studied area in the grid of 0.5 degrees of longitude and latitude, i.e., the velocity field has been estimated with half-degree steps in latitude and longitude using ANFIS. Also, in this figure, the GPS velocity field is shown in the position of the stations with black vectors.

In the testing step, the ANFIS model in case # 1 has the lowest RMSE and relative error. As a result, the estimating velocity vectors, in this case, are expected to be similar to GPS velocity fields in terms of direction and magnitude. In cases 2 and 3, the magnitude and direction of the velocity vectors obtained from the ANFIS are different from GPS.

In order to more accurately evaluate the output of the ANFIS model, the east–west component and north–south component of the estimated velocity field are shown in Fig. 8. This figure shows the earth's crust movement direction in the north–south and east–west directions.

Figure 8 shows the east–west and north–south components of the interpolated velocity field relative to the fixed frame of Eurasia. According to the figure, the amplitude of the east–west component is positive in the north, negative in the south, and zero in the center of the studied area. Also, the amplitude of the north–south component decreases from the south to the north. In the north–south component of the velocity field near the fault belt of Iran (the bold black line at the southwest), where the Arabian and Eurasian plates collide, the magnitude of the velocity field component is greater than that in other regions. In other words, in this area, the earth's crust bears a lot of pressure. Also, an increase in the velocity field can be seen in the north–south component in the northeast of the figure. In other words, the earth's crust in the northeast of the studied area tends to move toward the northeast. This result is in agreement with the result of Fig. 7 (velocity vectors obtained from the ANFIS), as well as the Raeesi et al. (2017) and Rastbood and Voosoghi (2012) studies.

After estimating the velocity field using the ANFIS (case # 1), the estimated velocity vectors are converted into the strain field and compared with the strains obtained from GPS. Figure 9 shows the comparison between the strains estimated by the ANFIS and OK models in the control stations AHAR (38.28° N, 47.06° E) and MNDB (36.74° N, 46.01° E) with the strain obtained from GPS. In this figure, co-directional vectors represent compressive strain and non-co-directional vectors represent tensile strain. For a clearer display, the strain vectors are displayed with 20 × zoom.

The compatibility of the strain field obtained from the ANFIS with the GPS strain is more than that of the OK model. The average correlation coefficient of the result of the ANFIS model at two control stations is 0.94, whereas for the OK model, the average correlation coefficient has been calculated at 0.88. In other words, the ANFIS has modeled the strain field variations with higher accuracy relative to the OK model. In both control stations, the compressive strain is dominant over the tensile strain, i.e., there

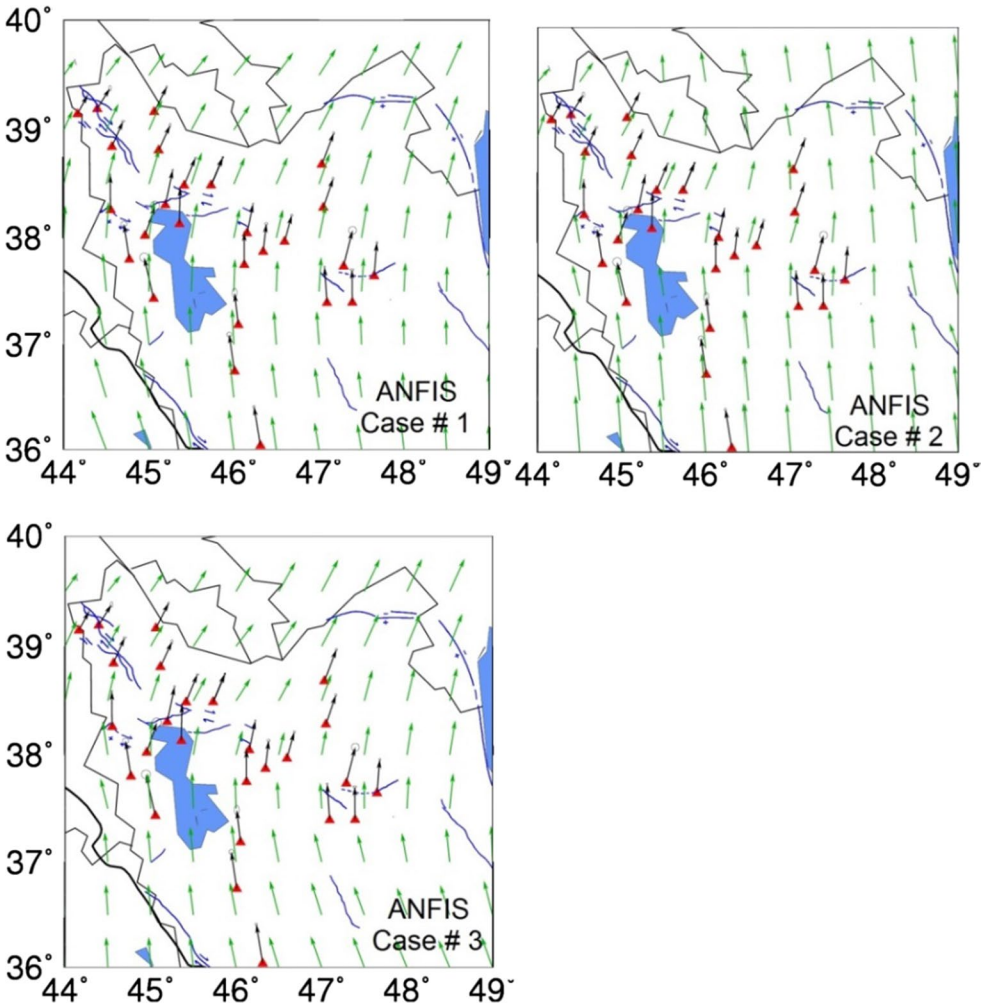

Fig. 7 Comparison of GPS velocity field (black vectors) and estimated velocity field using the ANFIS model (green vectors) for the three cases

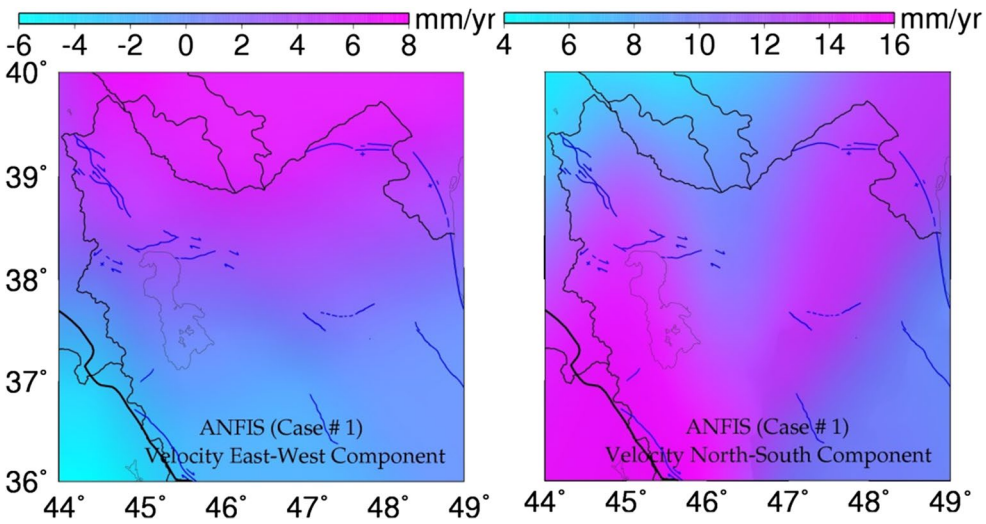

Fig. 8 East–west component (left panel) and north–south component (right panel) of estimated velocity field using ANFIS model at case # 1

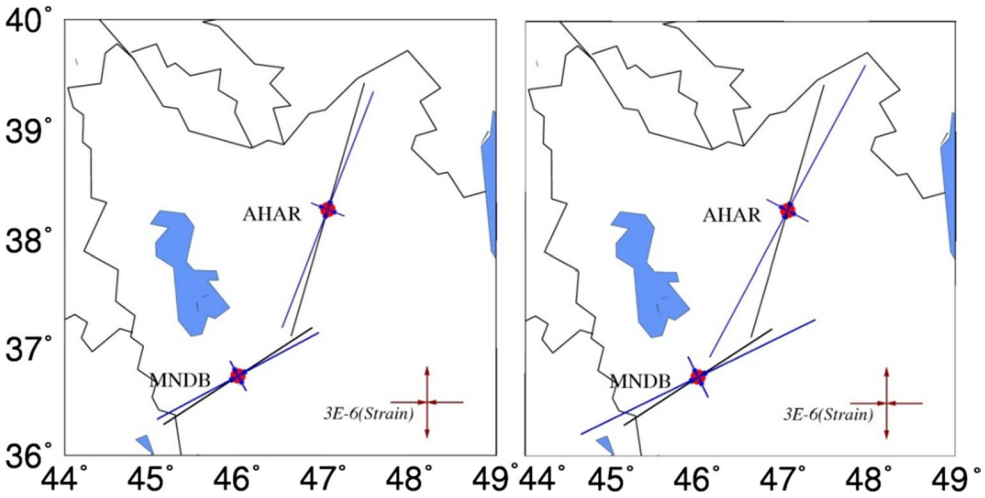

Fig. 9 Comparison of estimated strain field using ANFIS (left panel) and OK (right panel) models with GPS-derived strain field at two control stations AHAR and MNDB. Black vectors are the GPS strain and blue vectors show the ANFIS and OK strain fields

is strain accumulation in these two stations. The history of earthquakes in this area after the time span of observations (2007–2010) shows that an earthquake occurred in 2012 near the AHAR control station. In other words, strain accumulation can indicate movements in the earth's crust in the near future. The strains calculated by GPS are at the location of GPS stations.

While with the ANFIS model, the strain field can be estimated at other geodetic points of the studied network. The strain tensor components in each geodetic point within the studied network can be converted into surface dilatation, shear, and rotation rate. Then, based on these calculated parameters, the movement of the earth's crust can be interpreted.

Discussion

For a more accurate evaluation, the velocity vectors obtained by Raeesi et al. (2017), along with GPS and ANFIS velocity fields, are shown in Fig. 10.

Raeesi et al. (2017) used historical data from major earthquakes and GPS geodetic data to compute seismic strain rate, geodetic slip deficit, static stress drop, the magnitude frequency distribution parameters, and geodetic strain rate in the Iranian plateau to identify seismically mature fault segments and regions. The results of this research have been evaluated and confirmed with the velocity vectors obtained from GPS as well as with the geodynamic features of the Iranian plateau. Also, based on Rastbood and Voosoghi (2012), the Arabian plate exerted pressure on the Eurasian plate in the northeastern direction, and as a result, the overall movement of the Iranian plateau is in the north and northeast direction. The direction of the velocity vectors obtained from the ANFIS model in Fig. 10 is toward the north and

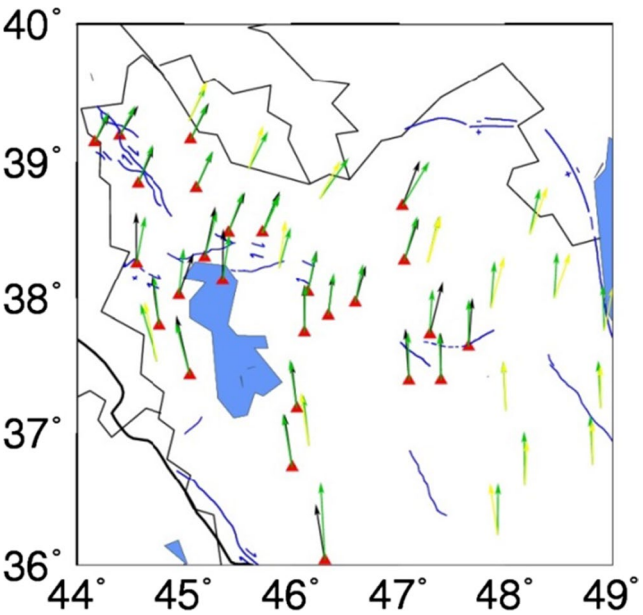

Fig. 10 Comparison of GPS velocity field (black vectors), estimated velocity field using ANFIS model (green vectors), and Raeesi et al. (2017) velocity field (yellow vectors)

northeast of the studied area. This result is consistent with that of Raeesi et al. (2017) and Rastbood and Voosoghi (2012).

According to the analysis, the averaged RMSE for the ANFIS, ANN, OK, and polynomial models in case # 1 (with the most training stations) is 1.6, 2.0, 2.7 and 3.2 mm/year, respectively. Also, the average relative error of models in case # 1 was computed at 6, 8, 13 and 15%, respectively. Comparing the RMSE and relative error of the ANFIS with other models in case # 1 showed that the accuracy of the proposed model is higher than other models. In cases 2 and 3, the RMSE of the proposed model was lower than other

models. However, the error of all four models increased compared to case # 1. In other words, all analyzed models show larger errors with decreasing number of training stations. The increase in the RMSE of the OK and polynomial models in cases 2 and 3 was more than that in case # 1. This shows that these two models require more training points in the training and parameter estimation steps.

After the training step of the ANFIS model, the velocity vectors are estimated at different points inside the network and compared with the GPS velocity field. The comparisons showed that in case # 1, the magnitude and direction of the velocity vectors estimated by the new model are in good agreement with the velocity vectors obtained from GPS. Also, comparing the velocity vectors estimated with the ANFIS with the velocity vectors obtained from this research conducted in the region shows their correct direction. The direction of the velocity vectors estimated with the new model is toward the northeast and consistent with the region's tectonic structure. After converting the velocity vectors into the strain field in the test stations AHAR and MNDB, a comparison was made with the strain field obtained from GPS. In this comparison, the strains estimated with the ANFIS agreed with GPS and correctly showed compression and tension directions. The estimated strains in two control stations with the new model represent strain accumulation. Strain accumulation can indicate the occurrence of an earthquake or strong displacement of a fault. Therefore, by estimating and studying the strains in different geodetic points, it is possible to discuss and investigate the accumulation of strains and the possibility of an earthquake or displacement of the earth's crust. This issue shows the effectiveness of the new model in geodynamic issues and earth's crust displacement analysis.

Conclusion

The idea of using the adaptive neuro-fuzzy inference system (ANFIS) to estimate the displacement field of the earth's crust was studied and analyzed as a new model. The novelty of this research was presenting a new idea for the continuous modeling of the velocity field of the earth's crust and, subsequently, the estimation of the strain field at different geodetic points within the network. Machine learning (ML) models have high computational speed, less mathematical complexity and high accuracy. As a result, the ANFIS model, which is a combination of artificial neural networks (ANN) and fuzzy logic, was used to model and estimate the displacement field. In order to evaluate the new method, the observations of 25 GPS stations in the northwest of Iran from 2007 to 2010 were used. Due to the availability of a complete set of GPS observations, as well as the active tectonic zone, this network was selected for evaluation. In the first step, the raw observations of the stations were processed in Bernese GNSS software and GPS velocity vectors were produced, fixed relative to the Eurasian plate. The velocity vectors obtained from GPS were considered as output to ANFIS, and the geodetic position of the GPS stations was the input variables of the model. In three cases with a different number of training and testing stations, the new model was evaluated. Also, at the test stations, the results of the ANFIS were compared with the GPS, ANN, Ordinary Kriging (OK), and polynomial velocity field.

The results showed that the ANFIS model has a high accuracy in estimating the velocity field of the earth's crust. This model can be the alternative of the OK and polynomial models to estimate the earth's crust velocity field continuously. Also, due to the high accuracy of the results of the ANFIS model in estimating the strain field, this model can be used in geodynamic research and analysis of fault movements in earthquakes. The need for a lot of training data is one of the disadvantages of the new model. Also, the speed of convergence to the optimal solution becomes extremely slow with increasing training data. In the continuation of this research, the geophysical parameters of the earth's crust can also be considered in the input vector, and the training of the model can be done with geometric and physical parameters.

Acknowledgements The authors thank the reviewers for providing very valuable and scientific comments. The National Cartographic Center (NCC) of Iran and the International GNSS Service (IGS) are also thanked for providing the required data.

Author contributions S.R. Ghaffari Razin initiated the study, provided the Matlab source codes for analysis, collected and analyzed the data. A. Rastbood and N. Hooshangi analyzed the part of data and wrote the manuscript. All authors helped to shape the analysis and manuscript. All authors reviewed the manuscript.

Data availability By contacting the corresponding author, all data can be provided to the readers. The IGS Rinex files can be downloaded from the ftp://cddis.gsfc.nasa.gov/pub/gps/data/daily.

Declarations

Conflict of interests The authors declare no competing interests.

References

Bogusz J, Klos A, Grzempowski P, Kontny B (2013) Modeling the velocity field in a regular grid in the area of Poland on the basis of the velocities of European permanent stations. Pure Appl Geophys 171(6):809–833. https://doi.org/10.1007/s00024-013-0645-2

Cakmakci M, Kinaci C, Bayramoğlu M, Yildirim Y (2010) A modeling approach for iron concentration in sand filtration effluent using adaptive neuro-fuzzy model. Expert Syst Appl 37(2):1369–1373

Chen R (1991) On the horizontal crustal deformations in Finland. Finish Geodetic Institute, Helsinki

Dach R, Hugentobler U, Fridez P, Meindl M (2007) Bernese GPS software version 5.0. Astronomical Institute, University of Bern, Bern

Djamour Y, Vernant P, Nankali H, Tavakoli F (2011) NW Iran-eastern Turkey present-day kinematics: results from the Iranian permanent GPS network. Earth Planet Sci Lett 307(1):27–34
Erdogan S (2010) Modeling the spatial distribution of DEM error with geographically weighted regression: an experimental study. Comput Geosci 36(1):34–43
Feizi R, Voosoghi B, Ghaffari RM, R, (2020) Regional modeling of the ionosphere using adaptive neuro-fuzzy inference system in Iran. Adv Space Res 65(11):2515–2528
Fernandez J et al (2018) Modeling the two- and three-dimensional displacement field in Lorca, Spain, subsidence and the global implications. Sci Rep 8(1):14782
Ghaderpour E, Pagiatakis SD, Hassan QK (2021) A survey on change detection and time series analysis with applications. Appl Sci 11(13):6141. https://doi.org/10.3390/app11136141
Ghaffari Razin MR, Voosoghi B (2020) Ionosphere time series modeling using adaptive neuro-fuzzy inference system and principal component analysis. GPS Solut 24(2):24–51
Ghaffari Razin MR, Voosoghi B, Mohammadzadeh A (2015) Efficiency of artificial neural networks in map of total electron content over Iran. Acta Geod Geophys 51(3):541–555
Grafarend EW, Voosoghi B (2003) Intrinsic deformation analysis of the earth's surface based on displacement fields derived from space geodetic measurements. Case studies: present-day deformation patterns of Europe and of the Mediterranean area (ITRF data sets). J Geod 77(5):303–326
Gullu M, Yilmaz I, Yilmaz M, Turgut B (2011) An alternative method for estimating densification point velocity based on back propagation artificial neural networks. Stud Geophys Geod 55(1):73–86
Hossainal MM, Becker M, Groten E (2010) Comprehensive approach to the analysis of the 3D kinematics deformation with application to the Kenai Peninsula. J Geod Sci 1(1):59–73. https://doi.org/10.2478/v10156-010-0008-1
Hu J, LiZ SQ, Zhu J, Ding X (2012) Three-dimensional surface displacements from InSAR and GPS measurements with variance component estimation. IEEE Geosci Remote Sens Lett 9(4):754–758. https://doi.org/10.1109/LGRS.2011.2181154
Jang JS (1993) ANFIS: adaptive-network-based fuzzy inference system. IEEE Trans Syst Man Cybern 23(3):665–685. https://doi.org/10.1109/21.256541
Joseph VR (2006) Limit Kriging. Technometrics 48(4):458–466
Konakoglu B (2021) Prediction of geodetic point velocity using MLPNN, GRNN, and RBFNN models: a comparative study. Acta Geod Geophys 56(2):271–291. https://doi.org/10.1007/s40328-021-00336-6
Li J, Heap AD (2008) A review of spatial interpolation methods for environmental scientists. Geoscience Australia, Canberra
Liang H, Zhan W, Li J (2021) Vertical surface displacement of mainland China from GPS using the multi-surface function method. Adv Space Res 68(12):4898–4915. https://doi.org/10.1016/j.asr.2021.02.024
Malekshahian Z, Raoofian Naeeni M (2018) Deformation analysis of Iran Plateau using intrinsic geometry approach and C1 finite element interpolation of GPS observations. J Geodyn 119(2018):47–61
Matheron G (1971) The theory of regionalized variables and its applications. Centre de Geostatistique, Fontainebleau Paris
Moghtased-Azar K, Zaletnyik P (2009) Crustal velocity field modeling with neural network and polynomials. In: Sideris MG (ed) Observing our changing, earth international association of geodesy symposia, pp 809–816
Raeesi M, Zarifi Z, Nilfouroushan F, Boroujeni S, Tiampo K (2017) Quantitative analysis of seismicity in Iran. Pure Appl Geophys 174(3):793–833
Rastbood A, Vosooghi B (2012) Study of tectonic plate motions contribution of the middle-east region in the GPS velocity field of Iranian campaign global geodynamic network scientific quarterly journal. Geosciences 21(84):15–24
Rumelhart DE, Hinton GE, Williams RG (1986) Learning internal representations by error propagation. In: Parallel distributed processing, MIT Press, Cambridge, pp 318–362
Segal P, Matthews MV (1988) Displacement calculations from geodetic data and the testing of geophysical deformation models. J Geophys Res 93(B12):14954–14966
Voosoghi B (2000) Intrinsic deformation analysis of the earth surface based on 3-D displacement fields derived from space geodetic measurements, PhD thesis, Department of Geodesy and Geoinformatics, Stuttgart University
Yetilmezsoy K (2019) Applications of soft computing methods in environmental engineering. In: Hussain C (ed) Handbook of environmental materials management. Springer, Cham
Yilmaz M (2013) Artificial neural networks pruning approach for geodetic velocity field determination. BCG Boletim De Ciências Geodésicas 19:558–573
Yilmaz M, Gullu M (2014) A comparative study for the estimation of geodetic point velocity by artificial neural networks. J Earth Syst Sci 123(4):791–808

Seyyed Reza Ghaffari-Razin received his Ph.D. degree in geomatics engineering from K.N.Toosi University of Technology, Tehran, Iran (2014–2017). Now, he is an assistant professor in the department of geoscience engineering at the Arak University of Technology. His main area of interest is atmospheric modeling and surface deformation analysis.

Asghar Rastbood received his Ph.D. in Geomatics Engineering from K. N. Toosi University of Technology, Tehran, Iran (2006–2011). Now he is an assistant professor in the faculty of Civil Engineering at the University of Tabriz. His main area of interest is space geodesy and geodynamic modeling.

Navid Hooshangi is an assistant professor in the department of geoscience engineering at Arak University of Technology , Arak, Iran. He received his Ph.D. degree in geomatics engineering from K.N.Toosi University of Technology. He is interested in Geographic information systems (GIS), Multi-agent system simulation, Uncertainty analysis, and spatial analysis.